

UNIVERSIDADE DO VALE DO RIO DOS SINOS - UNISINOS

Programa de Pós-Graduação em Geologia

Linha de Pesquisa: Estratigrafia e Evolução de Bacias

Seminário Final de Mestrado Acadêmico

Marlise Colling Cassel

**IMPLICAÇÕES PALEOAMBIENTAIS DOS FOLHELHOS NEGROS NA RAMPA
CARBONÁTICA DA FORMAÇÃO IRATI**

São Leopoldo, 12 de dezembro de 2017.

Marlise Colling Cassel

**IMPLICAÇÕES PALEOAMBIENTAIS DOS FOLHELHOS NEGROS NA RAMPA
CARBONÁTICA DA FORMAÇÃO IRATI**

Dissertação apresentada ao Programa de
Pós-Graduação em Geologia – Área de
Concentração, Geologia Sedimentar Linha de
Pesquisa Estratigrafia e Evolução de Bacias,
da Universidade do Vale do Rio dos
Sinos (UNISINOS), como parte das exigências
para a obtenção do título de Mestre em Geociências

Orientador: Prof. Dr. Ernesto Luiz Correa Lavina

Banca Avaliadora: Dr. Laury Medeiros de Araújo

Dr. Francisco M. W. Tognoli

São Leopoldo, 2017.

C344i

Cassel, Marlise Colling.

Implicações paleoambientais dos folhelhos negros na rampa carbonática da formação Irati / Marlise Colling Cassel. – 2017.

35 f. : il. ; 30 cm.

Dissertação (mestrado) – Universidade do Vale do Rio dos Sinos, Programa de Pós-Graduação em Geologia, 2017.

“Orientador: Prof. Dr. Ernesto Luiz Correa Lavina.”

1. Estratigrafia de alta resolução.
 2. Permiano.
 3. Bacias intracratônicas.
 4. Mesosaurus.
 5. Geoquímica orgânica.
 6. Espectroscopia gama.
 7. Anóxia.
- I. Sequências TR. I. Título.

CDU 55

Dados Internacionais de Catalogação na Publicação (CIP)
(Bibliotecário: Flávio Nunes – CRB 10/1298)

SUMÁRIO

APRESENTAÇÃO DA DISSERTAÇÃO.....	1
Introdução.....	1
Objetivo.....	2
Métodos.....	2
Resultados.....	3
MANUSCRITO.....	4
Abstract.....	4
1. Introduction.....	5
2. Methodology.....	6
3. Regional Geology.....	7
4. Results and interpretations.....	9
4.1 Depositional System.....	9
4.2 Organic matter, oxygenation and salinity (organic geochemistry and gamma spectrometry).....	11
4.3 Stratigraphic scheme of depositional sequences.....	14
4.4 High frequency cycles.....	16
5. Final considerations.....	17
References.....	19
Figure captions.....	26
Figure.....	28
SINTESE INTEGRADORA.....	35

APRESENTAÇÃO DA DISSERTAÇÃO

O estudo aqui apresentado é fruto do trabalho de mestrado executado na Universidade do Vale do Rio dos Sinos ao longo de dois anos, sob orientação do Professor Dr. Ernesto Lavina. A dissertação intitulada **IMPLICAÇÕES PALEOAMBIENTAIS DOS FOLHELHOS NEGROS NA RAMPA CARBONÁTICA DA FORMAÇÃO IRATI** tem seus resultados apresentados na forma de artigo científico intitulado: **PERMIAN CARBONATE RAMPS AND BLACK SHALES: PALEOENVIRONMENTAL DYNAMICS IN A RESTRICT BASIN.** O artigo apresenta um detalhamento das fácies e arcabouço estratigráfico da Formação Irati no sul da Bacia do Paraná, bem como inferências paleodeposicionais baseadas em análises de geoquímica orgânica e gamaespectrometria. Este artigo foi submetido ao periódico *Palaeogeography, Palaeoclimatology, Palaeoecology*, o qual pertence ao estrato A2 qualis CAPES. O trabalho tem a coautoria do orientador Dr. Ernesto L. C. Lavina e coorientadora Dra. Joice Cagliari, da Unisinos, e Dr. René Rodrigues e Dr. Egberto Pereira, da Universidade do Estado do Rio de Janeiro, com os quais desenvolveu uma parceria de trabalho.

Introdução

Estudos envolvendo a deposição de folhelhos pretos remetem, de forma recorrente, uma associação com eventos de escala global no passado geológico. Mudanças climáticas, perturbações no ciclo do carbono, até extinções em massa podem estar bem registradas em intervalos de folhelhos negros, sobretudo quando depositados em rampas carbonáticas. Dessa forma, unidades estratigráficas que contemplem tais registros se mostram como uma ótima oportunidade de investigação de fenômenos extremamente relevantes do passado.

A Formação Irati, além de corresponder a estes pré-requisitos é um marco na Bacia do Paraná, dada sua extensa lateralidade faciológica. Cabe salientar que também é relevante para todo o interior cratônico do Gondwana, na medida em que é síncrona com outros pacotes de folhelhos ricos em matéria orgânica presentes nas bacias Chaco-Paraná, Karoo e Kalahari.

Sabendo da necessidade de mais estudos, discussões e detalhamento da Formação Irati, devido sua grande distribuição areal e restritas áreas aflorantes, o estudo aqui apresentado espera contribuir com o arcabouço estratigráfico e enriquecer discussões já existentes acerca da dinâmica paleoambiental do Gondwana no Permiano.

Objetivo

A partir da contextualização do objeto de estudo (a Formação Irati), destacam-se questões para problematização deste tema (sua dinâmica paleoambiental): a) é possível delimitar a influência do clima no seu empilhamento sedimentar? b) como se dá a variação de salinidade e oxigenação do substrato?

Desta forma foi delimitado como objetivo deste trabalho detalhar a evolução paleoambiental da Formação Irati, tendo a salinidade e oxigenação do substrato como possíveis indicadores do clima.

Métodos

Para execução do trabalho foi necessária a descrição de testemunhos de sondagem, e perfis geofísicos de raios gama para correlação, que resultou na confecção de perfis litológicos e uma seção estratigráfica, cujo datum é o nível inferior de folhelhos negros. Estes compuseram o arcabouço estratigráfico analisado na perspectiva das sequências

depositionais. A partir de então foram feitas coletas para análises de geoquímica orgânica e uma medição gamaespectrométrica, com o fim de diferenciar os canais de potássio, urânio e tório. No corpo do artigo submetido ocorre o detalhamento das informações referentes aos materiais e métodos.

Resultados

Os resultados obtidos são apresentados na forma de artigo científico submetidos ao periódico Palaeogeography, Palaeoclimatology, Palaeoecology. Foi definido o sistema deposicional da Formação Irati como rampa carbonática com os domínios interno, médio e externo, como já proposto por Araújo (2001). O arcabouço estratigráfico foi detalhado em três sequências deposicionais e ciclos T-R de mais alta frequência. Com relação aos aspectos paleoambientais foram traçadas inferências quanto à natureza e teor de matéria orgânica presente. Os dados de geoquímica orgânica, aliados aos dados de gamaespectrometria permitiram traçar inferências paleoambientais que evidenciaram oscilações no clima por meio da variação entre períodos de menor e maior umidade, bem como de concentração e diluição da salinidade. Cabe ainda destacar o registro fossilífero de escamas de peixe e restos esqueletais de mesossaurídeos.

1 **Permian carbonate ramps and black shales: Paleoenvironmental dynamics in a restrict**
2 **basin**

3 Marlise Colling Cassel^{1*}, Ernesto Luiz Correa Lavina¹, Joice Cagliari¹, René Rodrigues²,
4 Egberto Pereira²

5 ¹*Universidade do Vale do Rio dos Sinos, Programa de Pós-Graduação em Geologia, Av.*
6 *Unisinos, 950, Cristo Rei, São Leopoldo, Rio Grande do Sul, CEP 92022-000, Brazil*

7 ²*Universidade do Estado do Rio de Janeiro, Departamento de Estratigrafia e Paleontologia,*
8 *Rua São Francisco Xavier, 524, Maracanã, Rio de Janeiro, Rio de Janeiro, Brazil*

9 Abstract

10 Bituminous shales have been associated to worldwide events, such as mass extinction and
11 anoxia, mainly when preserved in carbonate ramps, and constitute reliable records of this
12 dynamic. The Irati Formation is very suitable for the study of these intricate processes due to
13 the presence bituminous shales and carbonates. Based on core descriptions, gamma
14 spectrometry data (K, U, Th) and organic geochemistry (TOC, R_{ins}, S, IH and IO) a detailed
15 stratigraphic scheme was proposed for the southern sector of the basin. It is composed by
16 three depositional sequences formed internally by T-R cycles of highest frequency. The
17 analysis of the sedimentary facies demonstrated a carbonate ramp subdivided into outer,
18 middle and inner. It was possible to define a climatic control of the sea level changes and
19 climatic control, as well as oscillations in the salinity and oxygenation. The bituminous shales
20 record regular salinity levels, with dysoxia levels and even euxinia, associated to the increase
21 of the bioproductivity. The carbonate facies register periods of hypersalinity under oxic
22 environment, under semi-arid conditions. It was evidenced that the accumulation of
23 *Mesosaurus* skeletal remains results from the action of reworking fluxes, creating an endemic
24 facies in this region.

25 Key words: High resolution stratigraphy. Permian. Intracratonic basins. *Mesosaurus*.

26 TR sequences. Organic geochemistry. Gamma spectrometry. Anoxia

27 1. Introduction

28 Black shales have been associated to both regional and global geologic events, such as

29 climatic changes, oceanic anoxia and mass extinction (Phelps et al., 2015). Anoxic events

30 have been concomitant with significant perturbationn in the carbon global cycle, influencing

31 both the atmospheric and oceanic CO₂ concentration (Bonis et al., 2010; Phelps et al., 2015).

32 The most expressive records of these events are in carbonate platforms with occurrence of

33 abrupt changes between carbonatic facies and anoxic shales (Phelps et al., 2015).

34 In the middle and upper Permian, black shales have been studied under the

35 biogeochemical standpoint, because of the mass extinction at the end of this period (Wignall

36 and Twitchett, 1996; Clapham and Payne, 2011). Some models propose a physiologic crisis

37 resulting from the: pCO₂ and temperature increase stresses, associated to the pO₂ reduction

38 and carbonate saturation which caused acidification and environmental anoxia. Besides,

39 salinity changes are commonly associated to pCO₂ changes (Knoll et al., 2007).

40 In the Permian of the Paraná Basin and adjacent gondwanic basins of Chaco-Paraná

41 (Argentina), Karoo and Kalahari (Southern Africa) occurs thick packages of shales rich in

42 organic matter, intercalated with carbonatic layers (Oelofsen and Araújo, 1983; Oelofsen and

43 Araújo, 1987; Lavina, 1991; Hachiro, 1996; Milani et al., 1998Araújo, 2001). In the Permian

44 there are black shales in several basins of the cratonic interior of the South America which

45 respond to the same tecto-sedimentary cycle (Soares et al., 1974). This cycle of continental

46 expression is synchronous with huge sedimentary units of the center-east of the North

47 America, as proposed by Sloss (1963).

48 The Irati Formation is a suitable example to be studied as part of the worldwide
49 problematic aforementioned, since it has been deposited in the Middle Permian and is
50 composed by organic shales, siltstones and carbonates (Rocha-Campos et al., 2006; Santos et
51 al., 2006). Therefore, this formation can be a reliable register of the Permian environmental
52 dynamics which has been characterized by extreme events.

53 However, due to its broad area (around 2000 km in the N-S axis) and faciologic
54 variations associated to the outcropping area restricted shortly to the basin margin, the Irati
55 Formation still needs a further detailing in paleoenvironmental interpretations. Previous
56 studies have not reached agreement in paleoenvironmental aspects, being the salinity one of
57 the main topics of debate.

58 The main purpose of this work is the proposal a high-resolution stratigraphic scheme
59 for the bituminous shales and carbonates of the Irati Formation, and the analysis of its
60 paleoenvironmental meaning, based on geophysical and organic geochemistry approaches.
61 This analysis intends to bring a contribution to the understanding of the global paleoclimatic
62 dynamics due to the close relation between black shales and global events. Last but not least,
63 it will also contribute for the comprehension of both high frequency climatic and eustatic
64 controls.

65 2. Methodology

66 Twenty-three cores from the Brazilian Geological Survey (CPRM) were described and
67 analyzed in the southern part of Parana Basin (Fig. 3). The faciologic scheme obtained was
68 analyzed under the sequence stratigraphy standpoint, according to Hunt and Tucker's (1992)
69 model.

70 In two cores, samples for total organic carbon (TOC), total sulfur (S) and insoluble
71 residual have been collected each 60 cm core depth, totaling 214 samples, which have been

72 analyzed at *Laboratório de Estratigrafia Química e Geoquímica Orgânica da Faculdade de*
73 *Geologia, Universidade Estadual do Rio de Janeiro*. The R_{ins} was obtained by hot
74 acidification for elimination of carbonates. A LECO-COT502-308 equipment was used for
75 both TOC and S analyses. Subsequently, 52 samples have been chosen for pyrolysis-rock eval
76 analyses, which supplied hydrogen index (HI) and oxygen index (OI) values.

77 Additionally, new measurements in a gamma spectrometer RS 124 Radiation
78 Solutions, with a collect period of three minutes each 50 cm was conducted. This allowed the
79 differentiation of the potassium (K), thorium (Th) and uranium (U) channels and the
80 elaboration of new profiles, whose respective curves have been normalized to improve the
81 comparison of trends.

82 3. Regional Geology

83 The Paraná Basin is an intracratonic basin that spreads through the central-south
84 Brazilian territory, Northern Argentina, Paraguay and Uruguay, covering an area of 1 500,000
85 km² (Fig. 1). The Phanerozoic record reaches up to 8 km thick at its depocenter, ranging units
86 from the Late Ordovician to the Late Cretaceous (Fig. 2). The evolution of those units is
87 linked to uplifts and subsidence of orogenetic phases of the Southern Gondwana. The Paraná
88 Basin is subdivided into six supersequences: (i) Supersequence Rio Ivaí (Ordovician–
89 Silurian), (ii) Supersequence Paraná (Devonian), (iii) Supersequence Gondwana I
90 (Carboniferous–Lower Triassic), (iv) Supersequence Gondwana II (Triassic), (v)
91 Supersequence Gondwana III (Jurassic–Cretaceous) and (vi) Supersequence Bauru
92 (Cretaceous) (Zalan et al., 1990; Milani, 1997; Milani and Ramos, 1998; Cagliari et al., 2014)
93 (Fig. 1 and 2).

94 The Supersequence Gondwana I (Fig. 2) has a transgressive-regressive trend and a
95 gradual paleoenvironmental change, from glacially influenced at the bottom towards arid ones

96 in the top (Milani, 1997). The sedimentation begins with the glacial deposits of the Itararé
97 Group (Fig. 2). In the top of this group there is glacial conditions associated to the marine
98 transgression (Palermo and Rio Bonito formations) (Lavina and Lopes, 1987). The Rio Bonito
99 formation is composed of estuarine and deltaic deposits in the base, and facies of barrier-
100 beach with lagoon bodies and marshes associated (including thick coal layers). The
101 progressive relative sea level rising resulted in shoreface deposits (upper part of the Rio
102 Bonito Formation) and offshore of the Palermo Formation (Fig. 2). The adjacent unit (Iratí¹
103 Formation) is composed by siliciclastic deposits with intervals rich in organic matter,
104 carbonate and evaporites (Lavina, 1992). The Iratí Formation is overlain by the Serra Alta and
105 Teresina formations which represent the establishment of continental environments in the
106 basin. The top of this supersequence (Rio do Rasto and Pirambóia formations) represent non-
107 marine sedimentation, with lacustrine, fluvial and aeolian facies indicating the establishment
108 of arid conditions along the Mesozoic (Lavina, 1988; Lavina, 1992).

109 The Iratí Formation, of Artinskian age (278.4 ± 2.2 Ma) (Santos et al., 2006) has fine
110 siliciclastic sediments, occasionally rich in organic matter, intercalated with carbonates and
111 evaporites. The unit is divided into two members: Taquaral (lower) and Assistência (upper).
112 The first is composed by claystones and siltstones, while the second member has siltstones
113 and black shales, occasionally intercalated with carbonates (Mendes et al., 1966; Padula, 1968;
114 Petri and Coimbra, 1982; Oelofsen and Araújo, 1983; Lavina, 1992; Hachiro, 1996; Milani et
115 al., 1997; Araújo, 2001). In general terms, the sedimentation of the Iratí Formation is
116 considered as a marine restrict epicontinental environment, with salinity fluctuations,
117 substrate oxygenation and bioproductivity (Lavina, 1992; Hachiro, 1996; Araújo, 2001;
118 Rodrigues et al., 2010a; Rodrigues et al., 2010b). It is a depositional system of carbonate
119 ramp, divided into external, middle and inner ramps (Araújo, 2001). This association

120 represents the sedimentation during the restriction of the marine influx in the Paraná Basin
121 (Lavina, 1992; Milani et al., 1997).

122 The black shales and carbonates of the Assistência Member have been extensively
123 analyzed. They present high values of total organic carbon (TOC) up to 22% in the shales,
124 and the intercalated carbonate with low values of insoluble residues (Padula, 1968; Araújo,
125 2001; Rodrigues et al., 2010a; Rodrigues et al., 2010b; Alferes et al., 2011). The Assistência
126 Member is also characterized by the occurrence of skeletal remain of *Mesosaurus*, which can
127 be correlated to the Whitehill Formation, in the South Africa (Oelofsen and Araújo, 1983;
128 Oelofsen and Araújo, 1987; Lavina et al., 1991; Lavina, 1992; Soares, 2003).

129 4. Results and interpretations

130 4.1 Depositional System

131 The facies succession in the core description demonstrated the occurrence of a
132 carbonate ramp, as characterized by Burchette and Wright (1992), Wright and Burchette
133 (1996), Bosence and Wilson (2003), Miall (2010). This ramp is divided into outer, middle and
134 inner domains, all recorded in the deposits herein studied.

135 In the outer ramp (OR) domain, located below the level of the storm waves action,
136 predominates fine siliciclastic sediments, where may occur dysoxia. For the studied deposits
137 the following facies have been described: OR1) Black shale rich in organic matter (Fig. 4A).
138 Presents high peaks of TOC (around 20%), very high total S (1 to 3.5%) and R_{ins} around 75%
139 (Fig. 6); OR2) argillaceous siltstone with deep gray fissility, sometimes medium with
140 incipient lamination (Fig. 4B). It has rare fossiliferous levels with fish scales and crustaceans
141 in its upper part (Fig. 4F). The values of TOC are lower than 1%, the S ones are lower, and
142 the R_{ins} is high (85%) (Fig. 6); OR3) Siltstone gray with sparse wavy bedding planes of very
143 fine sandstone (Fig. 4C). It presents both TOC and S values very low, and R_{ins} values very

144 high (Fig. 6); OR4) Heterolithic claystone and very fine sandstone. Interbedding of gray
145 claystone with milimetric to centimetric lenses of fine sandstone occur (0.1 to 2 cm) (Fig.
146 4D). The claystone-sandstone contact is abrupt, being the sandstone and the claystone layers
147 truncated. The sandstone-claystone contacts, on the other hand, are either abrupt or
148 gradational. It has low TOC values, occasionally medium to high, with oscillatory pattern of S
149 and high values of R_{ins} (Fig. 6). In specific levels there are skeletal remains of *Mesosaurus*
150 (Fig. 4G). It is noteworthy that in 22 out the 23 cores described ribs, vertebrae, limb bones
151 and teeth of mesosaurids were found (Cassel and Lavina, 2013).

152 The physical processes involved in this domain are characterized by the predominance
153 of decantation. It has been identified, moreover, the influence of distal oscillatory fluxes and
154 reworking currents (bottom of storms), evidenced in the OR4 facies due to the disarticulation
155 of the bone fragments (Cassel and Lavina, 2013).

156 The middle ramp (MR) is composed by both carbonate and siliciclastic sedimentation,
157 whose alternance is typical of the study area. Occurs trough the gradation from claystone to
158 carbonate, corresponding to shallowing pulses (Fig. 4E). Other shallowing evidences have
159 also been found: tepee (Fig. 4H) and salt layer (Fig. 4I), similar to anhydrite nodules. Over
160 this interval there are carbonate with low angle, usually with wavy lamination on the top
161 (wave ripples and hummocky crossed stratification). The intercalated siliciclastic intervals are
162 composed of argillites, occasionally with layers of very fine sand and shale. Usually, present
163 low TOC with peaks oscillating toward higher values, but not exceeding 2%. The S is
164 variable but predominantly low, while the R_{ins} has a saw-pattern between 15% and 85% (Fig.
165 6).

166 The physical processes in this domain demonstrate the action of oscillatory fluxes,
167 reworking currents (either bottom or storms). In relation to the shallowing evidences found,
168 mainly the most intense (tepee), due to its low thickness and occasional occurrence, has also

169 been placed in the middle ramp. Being a ramp with smooth declivity, ephemeral relative sea
170 level oscillations may cause exposition even in this domain, as well as drownings.

171 The inner ramp (IR) is a shallow water environment of where carbonatic
172 sedimentation takes place, subjected to subaerial exposition. In the study area, it were
173 described carbonatic breccias with centimetric angulose clasts (Fig. 4E). The clasts of this
174 breccias present lamination in domic microrelief characteristic of microbialites (Araújo,
175 2001). The breccias and the V-shaped molds are evidences of subsequent aerial exposition.
176 They present low values of TOC and R_{ins} , and high values of S (Fig. 6).

177 4.2 Organic matter, oxygenation and salinity (organic geochemistry and gamma
178 spectrometry)

179 The TOC values of the Irati Formation are characterized by two aspects: Present levels
180 rich in organic matter (> 1%) (Arthur and Sageman, 1994) distributed along all the succession
181 and two anomalous occurrences of high peaks (around 20%) (Fig. 6).

182 The kerogen was characterized as type II, and subordinately as type III, through the IH
183 and IO data (Tissot and Welte, 1984) (Fig. 5). It was not recorded any abundance of organic
184 matter rich in lipidic fractions with H (the most reactive fraction) to reach Type I levels. This
185 means that the organic matter herein studied is either variably degraded, or of marine origin
186 (Type II) and subordinately continental (Type III), in a mixed or alternated pattern.

187 The IH/TOC graphic demonstrates an asymptotic pattern, where the increasing input
188 of organic matter is deprived of the corresponding increase in IH (Fig. 5). From this
189 asymptotic point onwards ($IH=300$ and $COT=4$), whose values belong to the bituminous shale
190 facies (OR1) (Fig. 4A), variations of the precursor source may occur, or delimitate the
191 beginning of the selective biodegradation. Palynological data indicate that from this TOC
192 level onwards (3% to 20%) occurs the highest amount of amorphous organic matter of the

193 interval, with significant content of H (Araújo, 2001). This demonstrates that the analyzed
194 kerogen comes from H-rich sources partially biodegraded, resulting in a kerogen fairly poor
195 in H (Type II).

196 In these organogenic layers, the data aforementioned, associated to the high values of
197 S indicate that the partial aerobic biodegradation of the organic matter in its movement along
198 the oxic water column is associated to the selective biodegradation of elements more
199 metabolizable (H) by sulphate reducing bacteria. At specific levels it was identified euxinic
200 environment in peaks of R_{ins} reduction (increase in the carbonate level) not common among
201 the bituminous shales, along with high values of S (Fig. 6). With the prerequisite of sulphate
202 availability dissolved in the water the metaboloc activity of the bacteria promotes the sulphate
203 reduction using the organic matter and generating bicarbonate and sulphidric acid, whose
204 presence characterize euxinic environments. This process of sulphate reduction raises the pH
205 and causes the precipitation of calcium carbonate. Data from biomarkers and isotopes confirm
206 the bacterial influence in the organic matter (Rodrigues et al., 2010a; Rodrigues et al., 2010b;
207 Alferes et al., 2011).

208 In relation to the points characterized as type III ($IH < 100$) and transitional II-III, these
209 occur in lower values of TOC (<2%) (Fig. 6), in fine siliciclastic facies (OR2 and OR4). In
210 these non-organogenic strata the low IH indicates mixture of different sources (both marine
211 and continental). The confirmation of this trend occurs by the predominance of allochthonous
212 palynomorphs (Araujo, 2001) and the correspondence to chemostratigraphic units which
213 indicate marine and terrestrial organic matter according to the biomarkers data (Rodrigues et
214 al., 2010a; Rodrigues et al., 2010b; Alferes et al., 2011). These data reinforce the increase of
215 the marine organic matter in relation to the continental one near to the SIM of the Irati A
216 Sequence.

217 The organic matter data aforementioned are in accordance to the level of oxygenation
218 of the substrate, since the preservation occurs under low levels. The U values of gamma
219 spectrometry identify less oxygenation beyond the levels enriched in organic matter. With the
220 disponibility of the ion U^{6+} soluble in seawater, in low oxygen levels occurs the reduction to
221 U^{4+} and precipitation as insolubles composts of uranium dioxide (UO_2) or hidroxides
222 ($U(OH)_4$) (Lünnings and Kolonic, 2003; Bonotto and Silveira, 2006). Levels of autogenic U
223 occur distributed along the studied section (Fig. 7). Besides the peaks of increase in the U
224 curve, the levels are easily seen in the Th/U curves where values near or below 2 indicate
225 anoxia, and in the curve of occurrence of authigenic U, which stresses the negative
226 covariation with the Th (in the form of monazite: resistate detritic mineral that depends of
227 allochthonous influx) (Fig. 7) (Andersson and Worden, 2004).

228 The S data supply not only information relative to the organic matter, but also salinity.
229 In the carbonatic strata occur very high S values (3.5) associated to low levels of TOC and
230 R_{ins} (Fig. 6). In these cases the increase of S is in accordance with the presence of sulphate
231 (gypsum and anhydrite), typical of evaporitic IR domains. Therefore the S, which has large
232 disponibility as sulphate dissolved in the sea water, becomes enriched in the inner part of the
233 ramp, as herein described associated to the IR and in thin and isolated levels of the MR. The
234 occurrence of salt layers with texture similar to anhydrite nodules, related to carbonatic strata
235 confirm the aforementioned data. These strata are probably correlated to carbonate associated
236 also to marine organic matter and hypersalinity conditions, according to isotope and
237 biomarkers data (Rodrigues et al., 2010a; Rodrigues et al., 2010b Alferes et al., 2011;). The
238 Th decrease, when associated to IR layers confirm the evaporitic conditions, demonstrating
239 the low humidity according to the reduction of continental detritic minerals input.

240 In relation to the salinity, besides the high levels herein registered, there are regular
241 salinity conditions in other intervals of the studied section. The values of U and S indicate

242 marine environment due to their infinite availability in the sea water. Th/U ratio with values
243 between 2 and 7 define oxic marine environment. Variation between this range predominate
244 in the succession (Fig. 7). Accordingly, S values even beyond the organogenic layers even
245 euxinic, present positive oscillations along the section (Fig. 7). The comparison of these
246 inferences to biomarkers data in other strata indicate normal salinity for other intervals of the
247 section (Rodrigues et al., 2010a; Rodrigues et al., 2010b Alferes et al., 2011).

248 4.3 Stratigraphic scheme of depositional sequences

249 Three depositional sequences have been identified in the studied interval, as
250 previously mentioned by Araújo (2001) and Hachiro (1996). However, a more detailed
251 register of the system tracts is herein proposed.

252 The Irati Sequence begins with a transgressive system tract (TST) characterized by the
253 succession of the facies OR3 and OR2 (Fig. 4), with reduction of the granulometry
254 representing a relative rise in the sea-level (Figs. 6). The subtle inflection of the TOC curve
255 towards higher values is in accordance to this trend, since it indicates either a reduction in the
256 oxygenation close to the substrate or the reduction in the siliciclastic input (Fig. 6). Above lies
257 the highstand system tract (HST), demonstrated by the increase of granulometry in the facies
258 OR4, which corresponds to a progradational trend (Fig. 6). The reduction in the
259 accommodation space associated to the smooth morphology of the ramp facilitated the
260 subaerial exposition even during the short relative sea level variations in this sector of the
261 ramp. In some cases it may cause pedogenetic processes.

262 On the top of this first sequence, where occurs the IR, it is recorded the forced
263 regression system tract (FRST), where the sea-level lowering allowed the development of
264 biotic activity typical of this type of ramp (Fig. 6). These microbialites are well indicated by
265 the low R_{ins} , demonstrating a high level of carbonates and low TOC, and suitable oxygenation

266 (Fig. 6). The abrupt contact of this level with the subjacent facies characterizes an erosive
267 surface of marine regression (Fig. 6). The subsequent formation of breccias in these deposits
268 demonstrates a relative sea level fall which caused subaerial exposition characterizing,
269 therefore, a sequence boundary (SB) (Fig. 6). Such boundary is identified in all the cores
270 described in the area. The occurrence, yet isolated, of bioturbation characteristic of excavation
271 in consolidated substrate reinforces this interpretation (Buatois et al., 2002).

272 The Irati B Sequence begins with a lowstand system tract (LST) characterized by the
273 occurrence of MR (Fig. 4E), where repetitive pulses of shallowing limited by adjacent
274 flooding surface are interpreted as lowstand parasequences (Fig. 6). This pattern is in
275 accordance to the R_{ins} curve which oscillates significantly, and some short and isolated peaks
276 of TOC increase (Fig. 6). At the top of this level the presence of sedimentary evidences of
277 oscillatory fluxes and reworking currents, as well as the increase in siliciclastics, indicates the
278 relative sea-level rise, which occur at the end of the lowstand system tract (Fig. 6). The
279 overlain transgressive system tract culminates in the facies OR1 of black shales (Fig. 4A),
280 which has a flooding surface easily identified in the gamma-ray logs and in the geochemical
281 indicators, especially the TOC between 16% and 20% (Fig. 6). This relative sea-level
282 indicates the restablishment of the OR (Fig. 6). The subsequent highstand system tract is
283 characterized by the reduction of the organic matter content in the shales, easily seen in the
284 TOC in the facies OR2 (Fig. 6). As observed in the previous sequence the contact with the IR
285 is abrupt and is again established an erosive surface of marine regression (Fig. 6). The forced
286 regression system tract is again characterized by the occurrence of bioherms. Subsequently,
287 the IR suffered subaerial exposition resulting in breccias, characterizing a sequence boundary.
288 It is important to mention that in the Irati B Sequence this system tract is not so expressive,
289 being thinner and absent in some cores.

290 The Irati C Sequence has in the base a lowstand system tract again characterized by
291 the occurrence of the MR, however thinner than in the previous sequence. Its carbonatic
292 sedimentation is evidenced in the R_{ins} curve (Fig. 6). The adjacent increase in the sea-level
293 rise characterize the transgressive system tract. This tract is demonstrated by the succession of
294 of OR4 and OR1 facies (Fig. 4D and 4A), with the predominance of the outer ramp, besides
295 the trend in the increase in the TOC values (Fig. 6). The reduction in the organic matter
296 amount in the subsequent unit (Serra Alta Formation), characterize the highstand system tract
297 (Fig. 5).

298 It is important to mention that previous studies have already made allusion to the
299 climatic control of facies succession in the Irati Formation, ascribing a 4th order hierarchy to
300 the cyclicity herein observed in the three depositional sequences (Araújo, 2010; Hachiro,
301 1996).

302 4.4. High frequency cycles

303 Cyclic transgressive-regressive (TR) internal oscillations have been observed along the
304 three depositional sequences (Fig. 7) according to Embry and Johannessen (1992). The
305 cyclicity was observed in the total curve of the gamma-ray log, whose radioactivity
306 corresponds to the sum of K, Th and U (Glover, 2012). In the case of siliciclastic rocks of fine
307 granulometry that represents the highest part of the succession herein described, the variations
308 of K are associated to the clay content of the rocks, indicating variations of higher and lower
309 energy in the environment due to oscillations in the water depth (Milani, 1997; Kearey et al.,
310 2009). Therefore, it is assumed that the increase in the K values correspond to a transgressive
311 trend. The detritic Th as mineral monazite resistates (Andersson and Worden, 2004; Kearey et
312 al., 2009), presents negative covariation with K, indicating higher energy intervals and
313 increased sedimentary input. On the other hand, in the cases of positive covariation with K,
314 the Th is associated to clay minerals by adsorption (Syed, 1999). In the case of U, due to its

315 behavior in relation to other radioactive elements, presenting negative covariation, it was
316 considered as authigenic, corresponding to low oxygenation contexts (as previously detailed).

317 The total amount of gamma ray is defined predominantly by the K, due to its relative
318 abundance in relation to the other radioactive elements measured. However, it is influenced
319 by the U and the Th, as negative covariations, reducing the effect of K in the total curve, as
320 well as positive covariation, which reinforce the effect of K in the curve.

321 Positive covariation was observed in eight out of nine analyzed cycles in the
322 succession, influenced predominantly by the K variation. Due to the affinity of U with low
323 oxygenation levels, such covariation suggests oxygen depletion in transgressive trends. The
324 increase peak of K with a negative covariation of U in the cycle eight demonstrates a rise in
325 the relative sea-level, without the establishment of low oxygenation context.

326 Besides the transgressive peaks indicated by K, there are also significant increase in
327 the U values that do not coincide with the K peaks and, therefore, are not conspicuous in the
328 total curve. These levels, which indicate low oxygenation, are not related with the sea level
329 rise. It was not observed covariation between U with TOC to justify the oxygen depletion by
330 events of productivity increase. Therefore, the peaks of authigenic U indicate climatic
331 changes which influenced the hydric imbalance and the circulation patterns.

332 As mentioned in the previous sub-item, the climate is the major controller of
333 sequences deposition in the 4th order scale (Araújo, 2010; Hachiro, 1996). Besides, it is
334 possible to infer that the cycles of highest frequency herein described, which are also mostly
335 influenced by the climate, are of 5th order hierarchy.

336 5. Final considerations

337 The depositional system of the Irati Formation was interpreted as a carbonatic ramp
338 with occurrence of three domains: inner, middle and outer. The succession of the domains is

339 controlled by the relative sea level changes which correspond to three depositional sequences
340 with TST, HSST, FRST and LSST. The depositional dynamics is complex and variable, since
341 it is influenced not only by oceanic incursions, but also the climate and, consequently the
342 continental input.

343 Along the section there are variations in the salinity and oxygenation of the substrate.
344 In general terms, there are predominance of normal salinity in the fine siliciclastic facies of
345 the OR both in the organogenic and in non-organogenic ones. In the carbonatic facies of the
346 IR and MR there are evidences of high salinity. There is also variations in the composition
347 of the organic matter. In the carbonatic facies of the IR and the MR the organic matter is of
348 marine origin. In the fine siliciclastic non-organogenic facies there are predominance of
349 marine organic matter, however with continental input. In the organogenic the precursors of
350 the organic matter are of bacterian origin.

351 This indicates different conditions of hydric imbalance. In two moments of the
352 sucession there was the establishment of an evaporitic environment in a semi-arid climate,
353 with low humidity and poor continental contribution. Such conditions are demonstrated in the
354 IR domain, associated to the RFST, where took place a microbial carbonatic sedimentation
355 under oxic conditions, in an environment of high salinity and subaerial exposition.

356 In the external ramp domain, associated to the TST developed an anoxic and euxinic
357 environment with normal salinity. This paleoenvironmental context resulted from the relative
358 sea level rise and increase in the productivity during phases of higher humidity.

359 It can be inferred that the factors that control the sedimentation are linked to
360 phenomena of 4th order. Near to the maximum flooding surface, the reduction of the
361 continental input demonstrates the predominance of allochthonous control (oceanic influx) in
362 the sea level oscillation in this sector of the basin in relation to the autochthonous control

363 (continental contribution). The 4th order cyclicity defines the relative sea level by eustatic
364 variations and climatic influence, as seen in oscillations between periods of low and high
365 humidity.

366 In relation to the high frequency cycles were observed T-R cycles identified in the
367 oscillations of the K amount, highlighted by the U increase. This indicates lower oxygenation
368 near to the substrate according to the transgressive trend. Besides the T-R cycles, the peaks of
369 U increase indicate phases of lower oxygenation beyond the transgressive trend. In these
370 cases of high frequency oscillation, the absence of relation with the TOC demonstrates the
371 climate as the controlling factor of the cycles.

372 In the case of oxygen depletion as evidenced by the absence of U in the transgressive peak the
373 climate influences the deposition by the interference in the hydric imbalance between the
374 continental input and the marine influx. This promotes the increase or reduction of the bottom
375 circulation due to the intermittent presence of thermohaline circulation, which reduces the
376 oxygen supply toward the substrate. In the case of T-R cycles evidenced by K the climatic
377 influence can even cause the increase in the thickness of the water column during the
378 transgressions.

379 It was noticed cyclicity in the deposition of the Irati Formation through the
380 depositional sequences and T-R cycles of highest frequency. Its hierarchy corresponds to
381 cycles of 4th and 5th order, respectively.

382 Referências

383 Alferes, C. L. F., Rodrigues, R., Pereira, E. 2011. Geoquímica orgânica aplicada à Formação
384 Irati, na área de São Mateus do Sul (PR), Brasil. Geochimica Brasiliensis, 25:47-54.

- 385 Andersson, P. O. D., Worden, R. H. 2004. Mudstones of the Tanqua Basin, South Africa: an
386 analysis of lateral and stratigraphic variations within mudstones, and a comparison of
387 mudstones within and between turbidite fans. *Sedimentology*, 51:479-502.
- 388 Araújo, L. M. (2001) Análise da Expressão Estratigráfica dos Parâmetros de Geoquímica
389 Orgânica e Inorgânica nas Sequências Depositionais do Iratí. Tese de Doutorado,
390 Universidade Federal do Rio Grande do Sul, Porto Alegre, 307 p.
- 391 Arthur e Sageman, 1994 Arthur, M. A., Sageman, B. B. 1994. Marine black shales:
392 depositional mechanisms and environments of ancient deposits. *Ann Rev Earth Planet
393 Sci* 22: 499–551.
- 394 Bonis, N. R., Ruhl, M., Kürschner, W. M. 2010. Climate change driven black shale
395 deposition during the end-Triassic in the western Tethys. *Palaeogeography,
396 Palaeoclimatology, Palaeoecology*, 290:151-159.
- 397 Bonotto, D. M., Silveira, E. G. 2006. Geoquímica do Urânio Aplicada a Águas Minerais, São
398 Paulo, Editora UNESP, 160 p.
- 399 Bosence, D. W. J., Wilson, R. C. L. 2003. Carbonate depositional Systems. In: Coe, A. L.
400 (ed.). *The Sedimentary Record of Sea-Level Change*. Cambridge, Cambridge
401 University Press, p. 209-274.
- 402 Buatois, L., Mángano, G., Aceñolaza, F. 2002. TrazasFósiles: señales de comportamiento
403 en el registro estratigráfico, 2.ed. esp. Museo Paleontológico Egidio Feruglio, Trelew,
404 382 p.
- 405 Burchette, T. P., Wright, V. P. 1992. Carbonate ramp depositional systems. *Sedimentary
406 Geology*, 79:3-57.

- 407 Cagliari, J., Lavina, E. L. C., Philipp, R. P., Tognoli, F. M. W., Basei, M. A. S., Faccini, U.
408 F.. 2014. New Sakmarian ages for the Rio Bonito formation (Paraná Basin, southern
409 Brazil) based on LA-ICP-MS U-Pb radiometric dating of zircons crystals. *Journal of*
410 *South American Earth Sciences*, 56: 265-277
- 411 Cassel, M. C., Lavina, E., L. 2013. Mortalidade de mesossaurídeos registrada em tempestitos
412 da Formação Irati (Permiano da Bacia do Paraná). In: XXIII Congresso Brasileiro de
413 Paleontologia, Anais, Gramado.
- 414 Clapham e Payne, 2011 Clapham, M. E., Payne, J. L. (2011) Acidification, anoxia, and
415 extinction: A multiple logistic regression analysis of extinction selectivity during the
416 Middle and Late Permian. *Geology*, 31(11):1059-1062.
- 417 Embry, A. F., Johannessen, E. P. 1992. T-R sequence stratigraphy, facies analysis and
418 reservoir distribution in the uppermost Triassic–Lower Jurassic succession, Western
419 Sverdrup Basin, Arctic Canada. In: Vorren, T. O., Bergsager, E., Dahl-Stamnes, O. A.,
420 Holter, E., Johansen, B., Lie, E., Lund, T. B. (eds.). *Arctic Geology and Petroleum*
421 *Potential*. Norwegian Petroleum Society, p. 121-146.
- 422 Glover, P. 2012, Petrophysics MSc Course Notes: Wire line logging.
- 423 Hachiro, J. 1996. O subgrupo Irati (Neopermiano) da Bacia do Paraná. Tese de Doutorado,
424 Universidade de São Paulo, São Paulo, 196 p.
- 425 Hachiro, J., Coimbra, M. C. 1992. Bonebeds e shellbeds como feições diagnósticas de
426 tempestitos da Formação Irati no Estado de São Paulo. In: 37º Congresso Brasileiro de
427 Geologia, Boletim de Resumos Expandidos, São Paulo, p. 511-512.
- 428 Hunt, D., Tucker, M. E., 1992. Stranded parasequences and the forced regressive wedge
429 systems tract: deposition during base-level fall. *Sedimentary Geology*, 81:1-9.

- 430 Hunt, D., Tucker, M. E., 1995. Stranded parasequences and the forced regressive wedge
431 systems tract: deposition during base-level fall – reply. *Sedimentary Geology*, 95:147-
432 160.
- 433 Kearey, P., Brooks, M., Hill, I. 2009. *Geofísica de Exploração*, São Paulo, Oficina de textos,
434 p. 391-398.
- 435 Knoll et al, 2007 Knoll, A. H., Bambach, R. K., Payne, J. L., Pruss, S., Fischer, W. W. (2007)
436 Paleophysiology and end-Permian mass extinction. *Earth and Planetary Letters*,
437 **256**:295-313.
- 438 Lavina, E. L. 1988. The PassaDois Group. In: Rocha-Campos, A. C. (ed.). *Gondwana Seven:*
439 Field excursion guide book. São Paulo, Universidade de São Paulo, p. 24-30.
- 440 Lavina, E. L. 1992. Geologia sedimentar e paleogeografia do Neopermiano e Eotriássico
441 intervalo Kazaniano-Scythiano) da Bacia do Paraná. Tese de Doutorado, Universidade
442 Federal do Rio Grande do Sul, Porto Alegre, 333 p.
- 443 Lavina, E. L., Araújo-Barberena, D. C., Azevedo, S. A. 1991. Tempestades de Inverno e Altas
444 Taxas de Mortalidade de Répteis Mesossauros. Um exemplo a Partir do Afloramento
445 Passo de São Borja, RS. *Pesquisas*, 18(1):64-70.
- 446 Lavina, E. L., Lopes, R. C. 1987. A transgressão marinha do Permiano Inferior e a evolução
447 paleogeográfica do Supergrupo Tubarão no Estado do Rio Grande do Sul. *Paula-*
448 *Coutiana*, 1:51-103.
- 449 Lünnig, S., Kolonic, S. 2003. Uranium spectral gamma-ray response as a proxy for organic
450 richness in black shales: applicability and limitations. *Journal of Petroleum Geology*,
451 26(2):153-174.

- 452 Mendes, J. C., Fulfaro, V. J., Amaral, S. E., Landim, P. M. B. 1966. A Formação Irati
453 (Permiano) e fácies associadas. Boletim da Sociedade Brasileira de Geologia,
454 15(3):23-43.
- 455 Miall, A. D. 2010. Sequence Stratigraphy. In: Miall, A. D. Principles of Sedimentary Basin
456 Analysis, 3.ed. Berlin, Springer, p. 320-379.
- 457 Milani, E. J. 1997. Evolução tectono-estratigráfica da Bacia do Paraná e o seu relacionamento
458 com a geodinâmica fanerozóica do Gondwana sul-ocidental. Tese de Doutorado,
459 Universidade Federal do Rio Grande do Sul, Porto Alegre, 255 p.
- 460 Milani, E. J., Faccini, U. F., Scherer, C. M., Araújo, L. M., Cupertino, J. A. 1998. Sequences
461 and stratigraphic hierarchy of the Paraná Basin (Ordovician to Cretaceous), Souther
462 Brazil. Boletim IG, Série Científica (29):125-173.
- 463 Milani, E. J., Ramos, V. A., 1998. Orogenia paleozoicas no domínio sul-ocidental do
464 Gondwana e os ciclos de subsidência da Bacia do Paraná. Revista Brasileira de
465 Ciências, 28(4):473-484.
- 466 Oelofsen, B., Araújo, D. C. 1983. Palaeoecological implications of the distribution of
467 mesosaurid reptiles in the permianIrati Sea (Paraná Basin), South America.
468 RevistaBrasileira de Geociências, 13(1):1-6.
- 469 Oelofsen, B., Araújo, D. C. 1987. Mesosaurustenuidens and Stereosternumtumidum from the
470 Permian Gondwana of both Southern Africa and South America. South
471 AfricanJournalof Science, 83:370-372.
- 472 Padula, V. T. 1968. Estudos geológicos da Formação Irati, sul do Brasil. Boletim Técnico da
473 Petrobrás, 11(3):407-430.

- 474 Petri, S., Coimbra, A. M. 1982. Estruturas sedimentares das Formações Irati e Estrada Nova
475 (Permiano) e sua contribuição para elucidação dos seus paleoambientes geradores,
476 Brasil. In: 5º Congresso Latinoamericano de Geologia, Actas, Buenos Aires, p. 353-
477 371.
- 478 Phelps, R. M., Kerans, C., Da-Gama, R. O. B. P., Jeremiah, J., Hull, D., Loucks, R. G. 2015.
479 Response and recovery of the Comanche carbonate platform surrounding multiple
480 Cretaceous oceanic anoxic events, northern Gulf of Mexico. *Cretaceous Research*,
481 54:117-144.
- 482 Rocha-Campos et al, 2006 Rocha-Campos, A.C., Basei, M.A.S., Nutman, A.P. e Santos,
483 P.R. 2006. Shrimp U-Pb Zircon geochronological calibration of the Late Paleozoic
484 Supersequence, Paraná Basin, Brazil. 5º South American Symposium on Isotopic
485 Geology (Punta del Este), Short Papers pp. 298–301.
- 486 Rodrigues, R., Pereira, E., Bergamaschi, S., Aferes, C. L. F. 2010a. Carbon Isotope
487 Stratigraphy of Organic Mater: Irati Formation, Lower Permian of Paraná Basin. In:
488 VII Simpósio Sul Americano de Geologia Isotópica, Anais, Brasília, p. 1.
- 489 Rodrigues, R., Pereira, E., Bergamaschi, S., Chaves, H. A. F., Alferes, C. L. F. 2010b.
490 Organic Geochemistry of Irati Formation, Lower Permian of Paraná Basin. In: XII
491 Congresso Latinoamericano de Geoquímica Orgânica, Memórias, Montevideo, p. 42-
492 43.
- 493 Santos, V. R., Souza, P. A., Alvarenga, C. J. S., Dantas, E. L., Pimentel, M. M., Oliveira, C.
494 G., Araújo, L. M., 2006. Shirimp U-Pb zircon dating and palynology of bentonitic
495 layers from the Permian Irati Formation, Paraná Basin, Brazil. *Gondwana Research*,
496 9:456-463.

- 497 Sloss, L. L. 1963. Sequences in the cratonic interior of North America. Geological Society of
498 America Bulletin, 74:93-114.
- 499 Soares, P. C., Landim, P. M. B., Fúlfaro, V. J. 1974. Avaliação preliminar da evolução
500 geotectônica das bacias intracratônicas brasileiras. In: 28º Congresso Brasileiro de
501 Geologia, Anais, Porto Alegre, p. 61-63.
- 502 Soares, M. B., 2003. A taphonomic model for the Mesosauridae assemblage of the Iriti
503 Formation (Paraná Basin, Brazil). *GeologicaActa*, 1(4):349-361.
- 504 Syed, A. S. 1999. Comparison studies adsorption of thorium and uranium on purê clay
505 minerals and local Malaysian soils sediments. *Journal of Radioanalytical and Nuclear
506 Chemistry*, 241(1):11-14.
- 507 Tissot e Welte, 1984 TISSOT, B. P., WELTE, D. H. *Petroleum Formation and Occurrence*.
508 Springer-Verlag. New York: 1984. 699 p.
- 509 Wignall, P. B., Twitchett, R. J. 1996. Oceanic anoxia and the End Permian mass extinction.
510 *Science*, 272:1155-1158.
- 511 Wright, V. P., Burchette, T. P. 1996. Shallow water carbonate environments. In: Reading, H.
512 G. (ed.). *Sedimentary Environments: Process, facies and stratigraphy*, 3.ed. Oxford,
513 Blackwell, p. 325-391.
- 514 Zalan, P.V., Wolff, S., Conceição, J.C. de J., Marques, A., Astolfia, M.A.M., Vieira, I.S.,
515 Appi, V.T., Zanotto, O.A., 1990. Bacia do paraná. In: Raja Gabaglia, G.P., Milani, E.J.
516 (Eds.), *Origem e evolução de bacias sedimentares*. Gávea, Rio de Janeiro, pp. 135-
517 168.
- 518

Figure captions

Fig. 1. Simplified geologic map of the Paraná Basin showing the structural outline of the basement, units and distribution of the supersequences described in the text (adapted from Milani, 1997).

Fig. 2. Stratigraphic diagram of the Gondwana I Supersequence, showing the 2nd order stratigraphic surfaces (adapted from Milani, 1997). In evidence is the level of Irati Formation.
*CB – Corumbataí Formation, whose age is equivalent to the Serra Alta and Teresina formations.

Fig. 3. Geographic localization of the study area with the lithoestratigraphic unit and the cores described.

Fig. 4. Photos of the facies described and commented along the text. A) Facies OR1 of black shales. B) Facies OR 2 of deep gray argillaceous-siltstone with fissility and incipient lamination. C) Facies OR3 of light gray siltstone. D) Heterolithic Facies OR4. E) The OR level is in dashed, overlain by the MR in continuous line. F) Fossiliferous level with fish sacales of the OR2 facies. G) Fossiliferous level with *Mesosuarus* remains of the OR4 facies. H) Tepee of MR shallowing. I) Salt layer similar to anhydrite nodules in the MR.

Fig. 5. Left: Correlation graphics of the oxygen index (IO) and hydrogen index (IH) of two probing and their resulting kerogen compositional fields. Right: Correlation graphics o total

organic carbon (TOC) and IH, a standard line demonstrating the asymptotic behaviour in the cluster.

Fig. 6. Lithologic and stratigraphic profile of two described cores showing the depositional sequences, their system tracts, the domains of the carbonatic ramo and the curves resulting from the geochemical analyses of the total organic carbon (TOC), sulphur (S), hydrogen index (HI) and insoluble residue (R_{ins}).

Fig. 7. Stratigraphic and lithologic profiles of the core described with gamma spectrometry, showing the total amount curve of gamma ray and the differentiable channels (U, Th, K), and derivative ratios. In the gamma ray curve (total) the cycles T-R are highlighted.

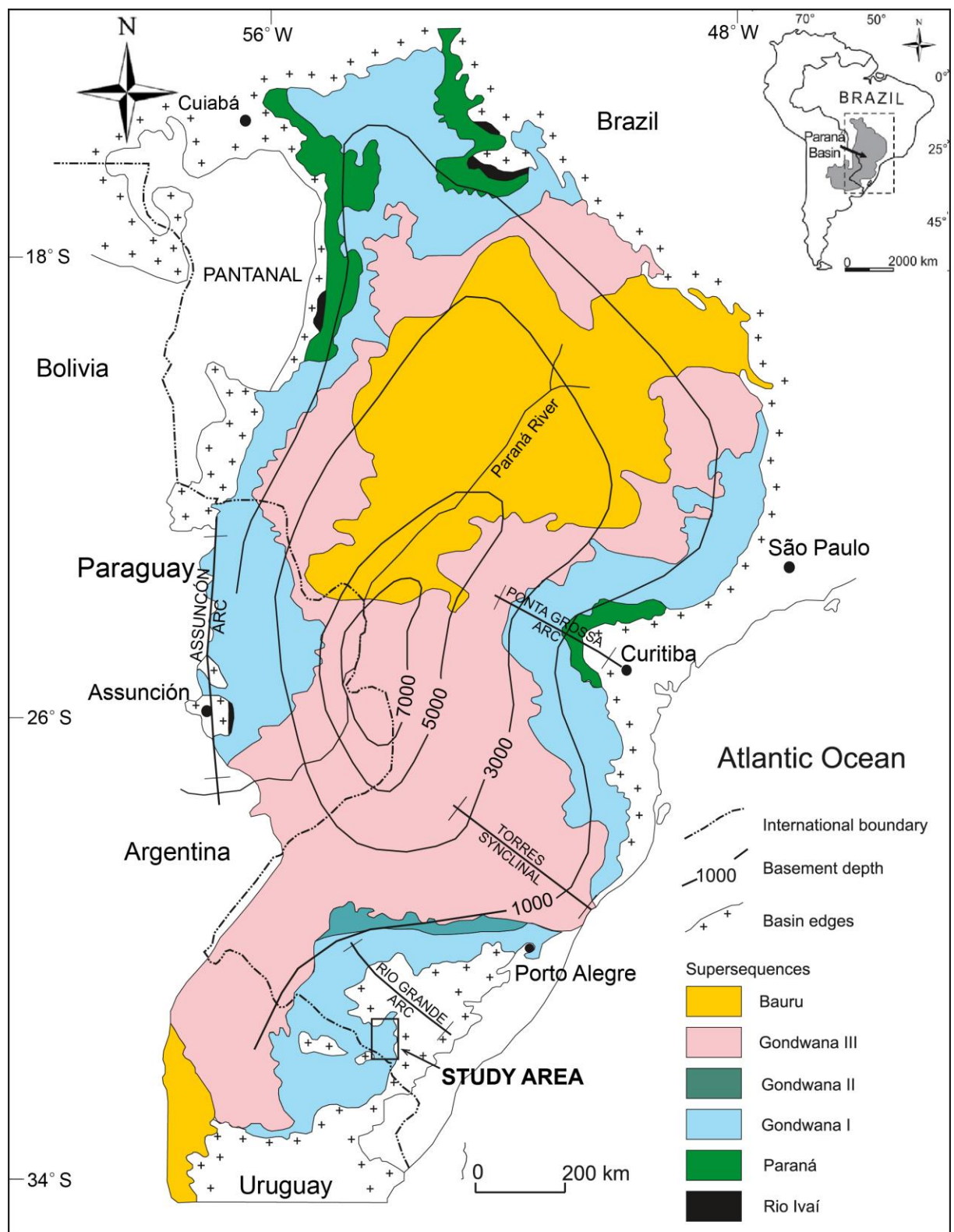


Fig. 1

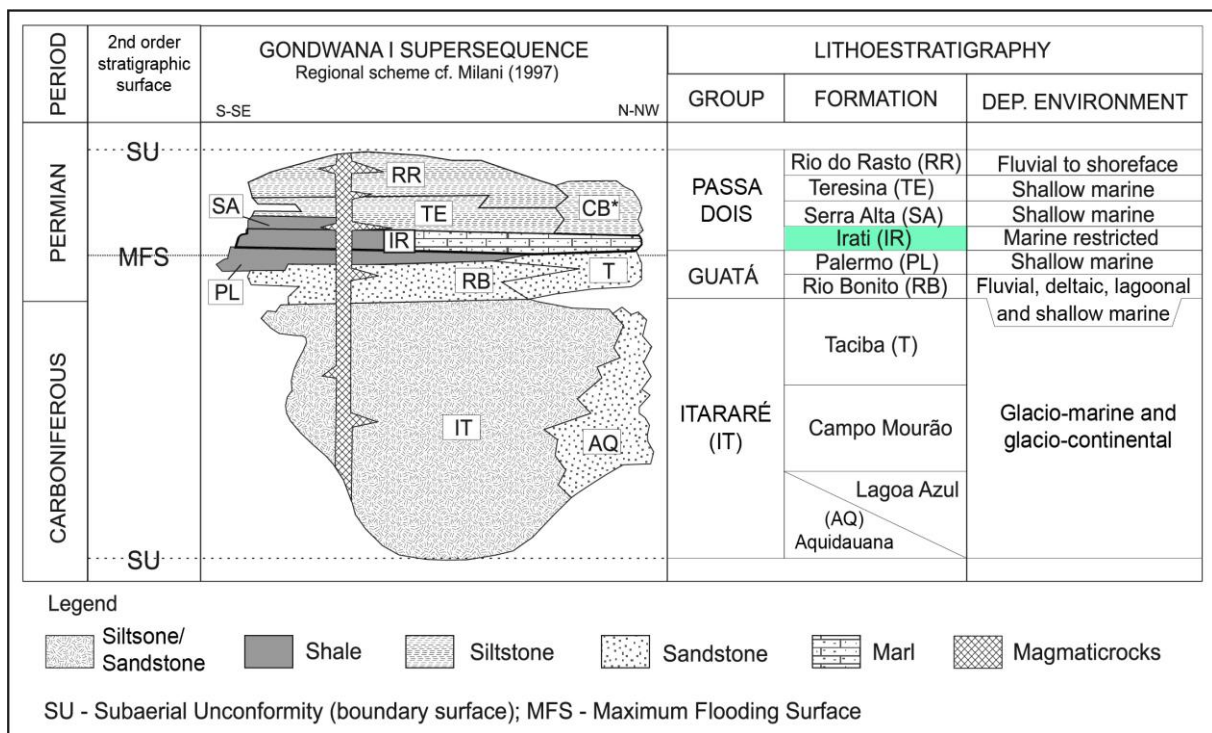


Fig. 2.

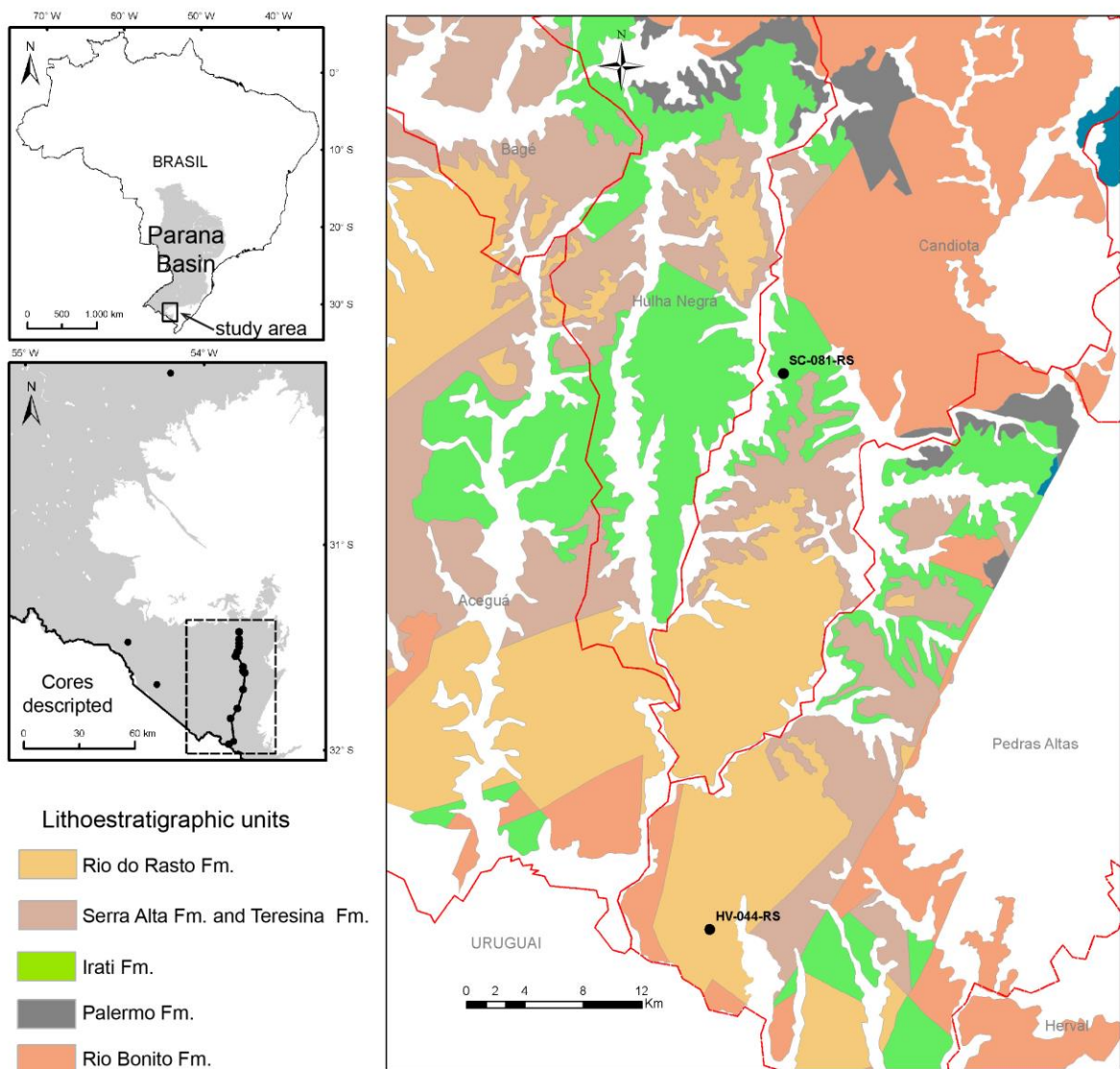


Fig. 3

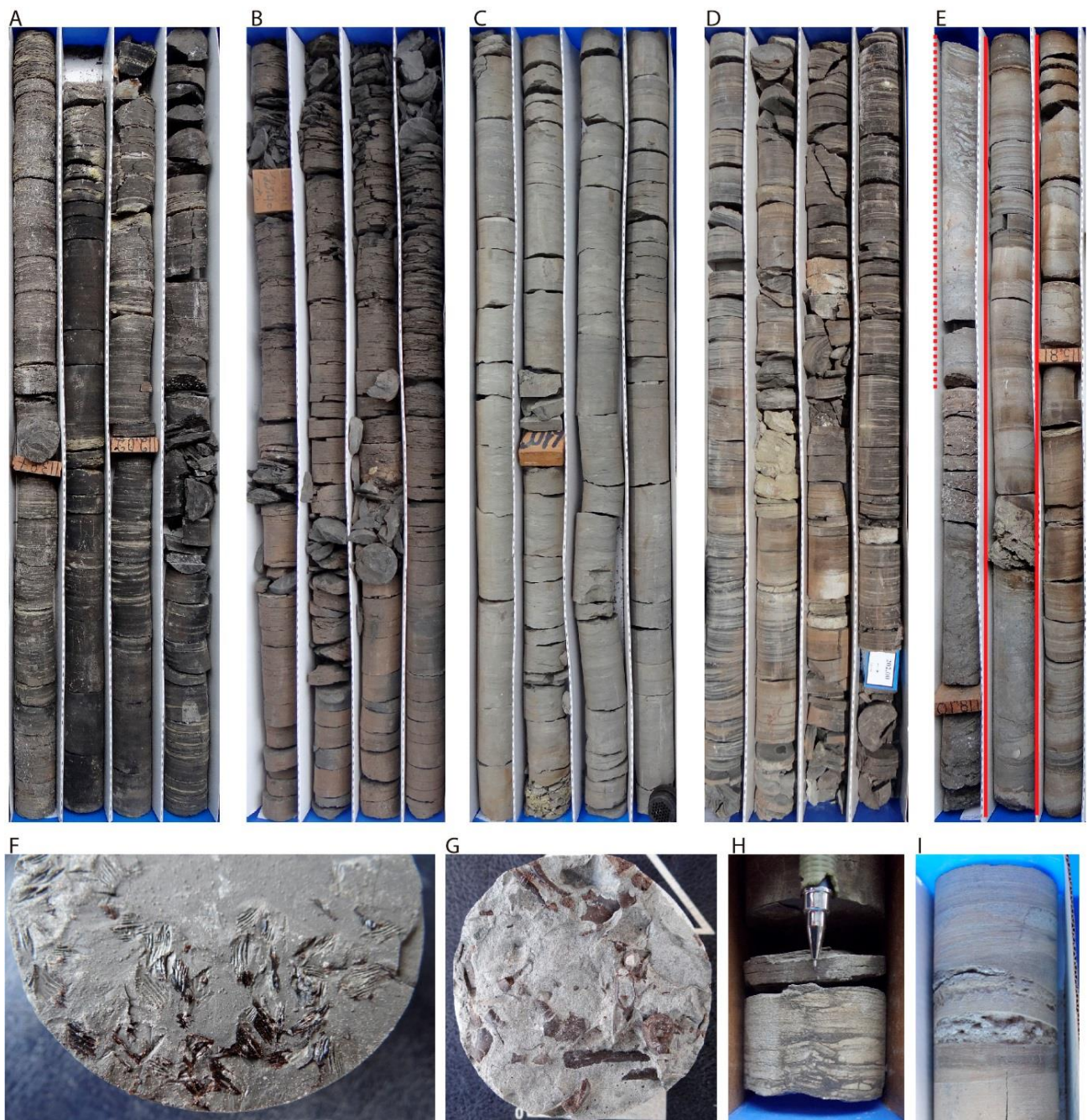


Fig. 4.

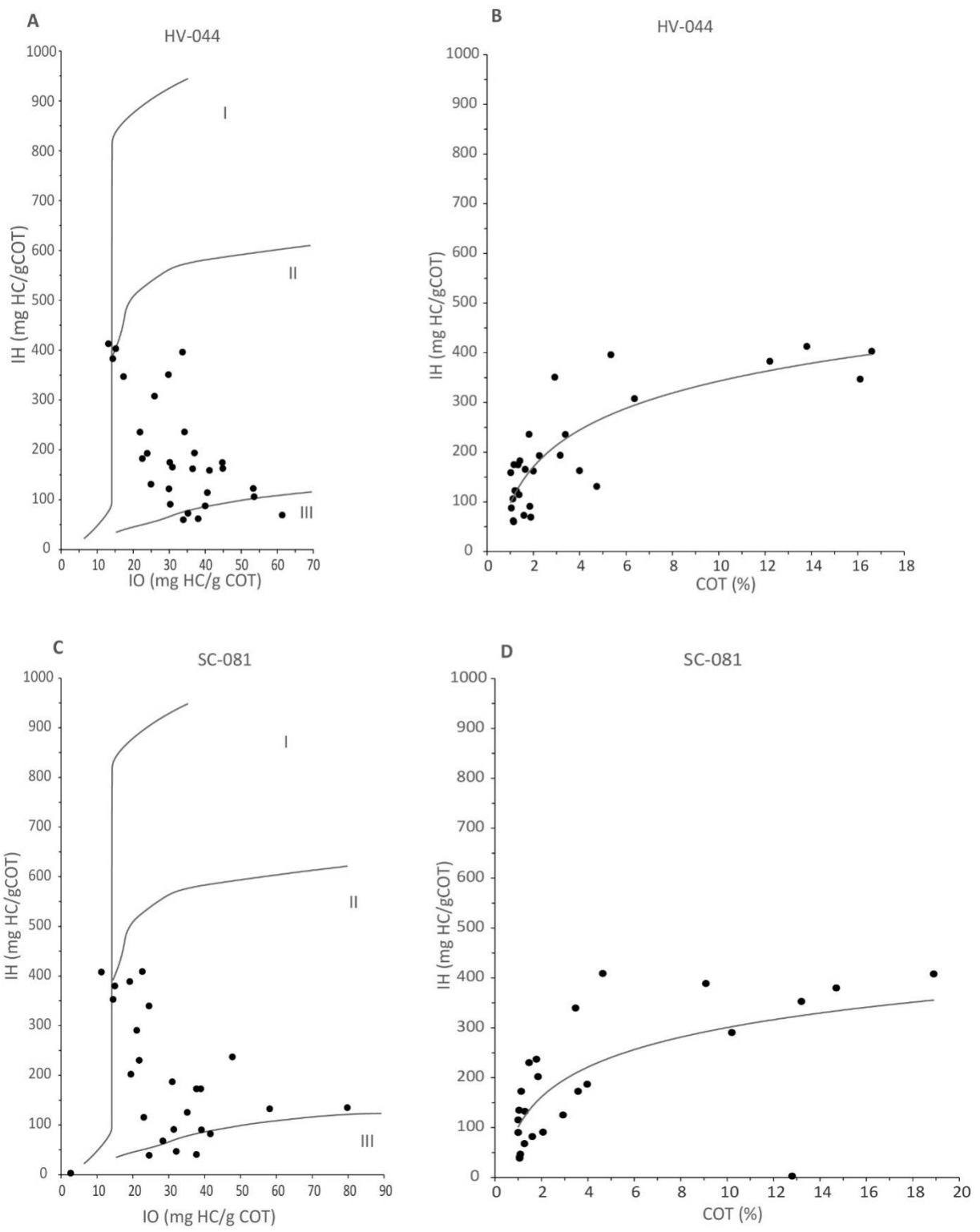


Fig. 5.

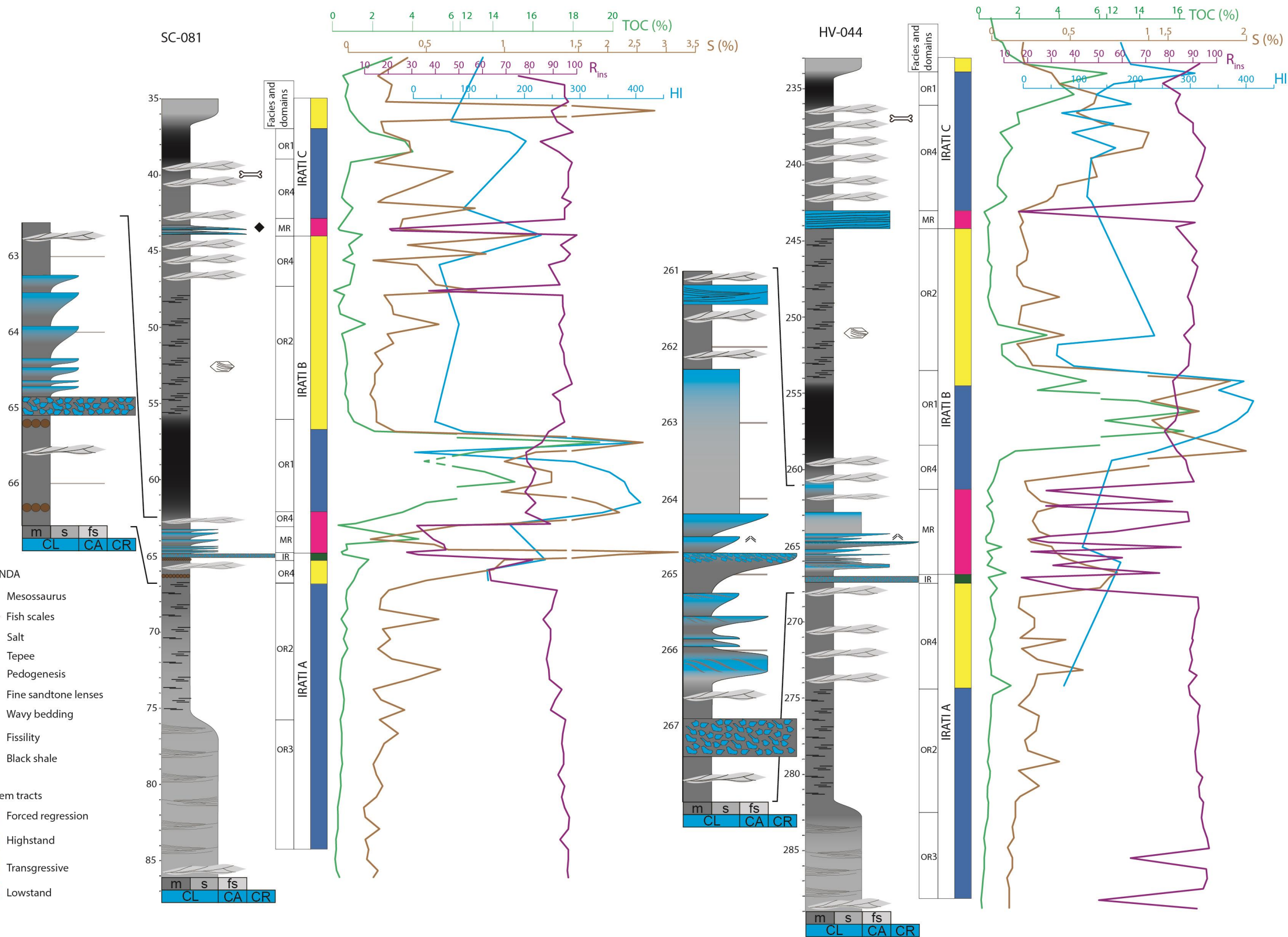


Fig. 6.

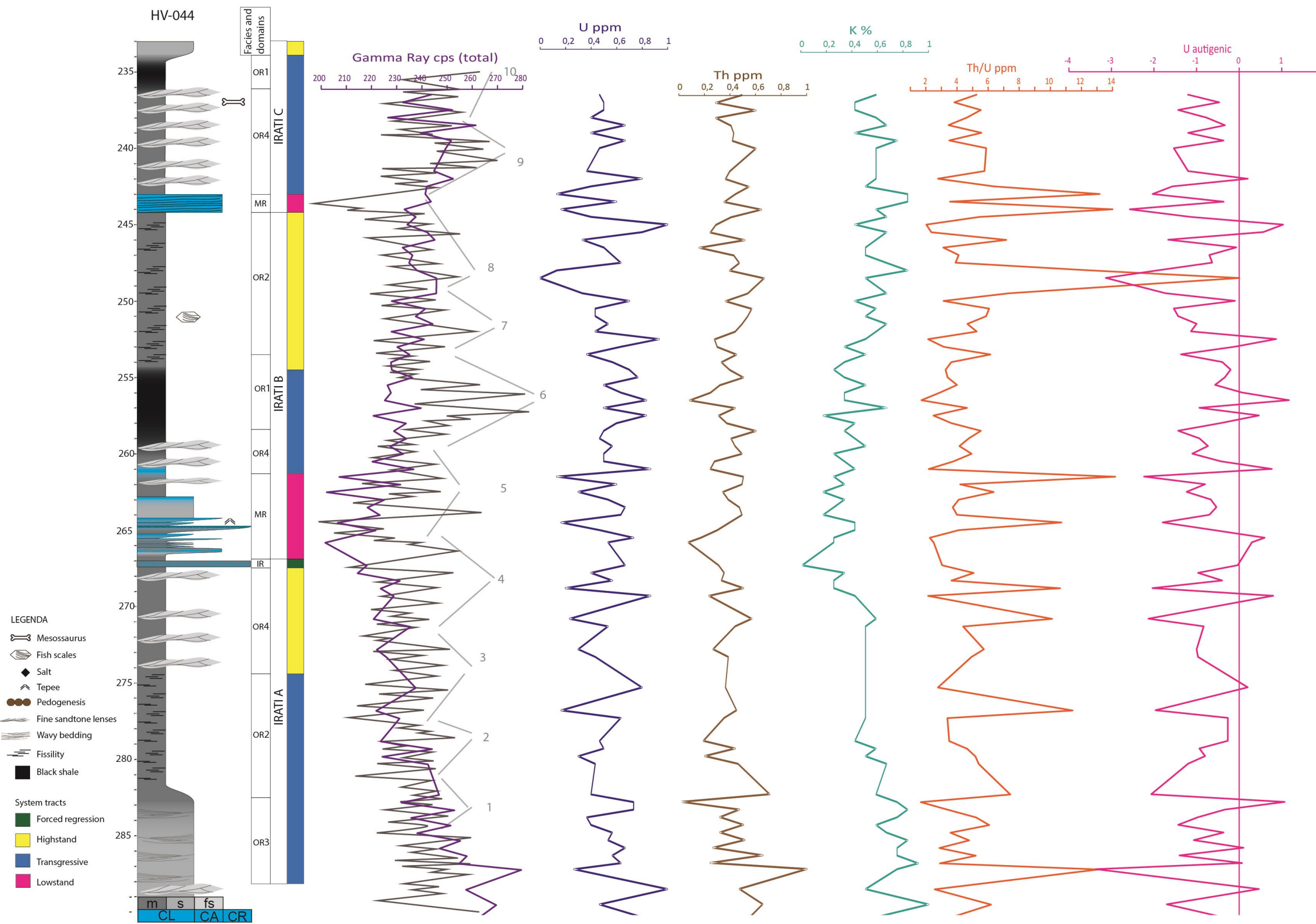


Fig. 7.

SÍNTESE INTEGRADORA

As inferências paleoambientais discorreram acerca da alternância de períodos úmidos e semi-áridos, associados a oscilações entre concentração e diluição salina, e oxigenação do substrato, que ocorreram ao longo do empilhamento das fácies de folhelhos, folhelhos betuminosos e carbonatos. Este resultado constituiu o contexto final do trabalho. Neste contexto também foi feita a caracterização da matéria orgânica presente na Formação Iratí, a qual se configura de forma heterogênea como marinha, bacteriana e até com níveis continentais. Para chegar a tais conclusões foi feito uso de ferramentas de geoquímica orgânica. Por outro lado, também no contexto mais adiante do presente trabalho, foi possível problematizar as hierarquias da ciclicidade presente nas sequências deposicionais e nos ciclos T-R, correspondendo a quarta e quinta ordem, respectivamente. Esta etapa contou com os dados detalhados de gamaespectrometria.

Para acessar esta instância de resultados, antes do ferramental analítico de laboratórios, foi necessário o domínio do arcabouço faciológico e estratigráfico da Formação Iratí no setor sul da Bacia do Paraná. Tal etapa só foi possível por meio da descrição de um considerável número de testemunhos de sondagem, bem como correlação com perfis geofísicos de outras sondagens para obter o controle lateral das fácies. Fruto desta etapa foi a caracterização do sistema deposicional como rampa carbonática, composta pelos domínios externo, médio e interno. A análise do empilhamento das fácies permitiu delimitar três sequências deposicionais, que compuseram a posterior problematização das hierarquias.

Desta forma, por meio desta síntese integradora nota-se que os resultados alcançados foram capazes de contemplar o que inicialmente foi proposto nos objetivos. O cenário paleoambiental da Formação Iratí no sul da Bacia do Paraná, apresentado neste estudo, pode alimentar as discussões acerca da dinâmica ambiental do Permiano.